Near Real-Time Wildfire Management Using Distributed Satellite System

Kathiravan Thangavel, Dario Spiller, *Member, IEEE*, Roberto Sabatini, *Senior Member, IEEE*, Pier Marzocca, and Marco Esposito

***Abstract*— Climate action (SDG-13) is an integral part of the Sustainable Development Goals (SDGs) set by the United Nations (UN), and wildfire is one of the catastrophic events related to climate change. Large-scale forest fires have drastically increased in frequency and size in recent years in Australia and other nations. These wildfires endanger the forests and urban areas of the world, demolish vast amounts of property, and frequently result in fatalities. There is a requirement for real-time/near real-time catastrophic event monitoring of fires due to their growing frequency. In order to effectively monitor disaster events, it will be feasible to manage them in real time or near real time due to the advent of the Distributed Satellite System (DSS). This research examines the possible applicability of DSS for wildfire surveillance. For spacecraft to continually monitor the dynamically changing environment, satellite missions must have broad coverage and revisit intervals that DSS can fulfill. A feasibility analysis, as well as a model and scenario prototype for a satellite artificial intelligence (AI) system, is included in this letter to enable prompt action and swiftly provide alerts. In our previous research, it is shown that on-board implementation, i.e., data processing utilizing hardware accelerators, is feasible. To enable Trusted Autonomous Satellite Operation (TASO), the same will be included in the proposed DSS architecture, and the outcomes will be provided. To demonstrate the applicability, the suggested DSS architecture will be tested in several geographic locations to demonstrate the system-wide coverage.**

***Index Terms*— 1-D convolutional neural network (CNN), climate action, Distributed Satellite System (DSS), edge computing, hardware accelerators, real-time monitoring, Sustainable Development Goal (SDG)-13, Trusted Autonomous Satellite Operation (TASO), wildfire.**

I. Introduction

CLIMATE change, as well as other human-caused factors, had a major impact on the ecosystem in recent years [1]. Extreme weather occurrences, droughts, dust storms, rising ocean levels, tornadoes, and wildfires are just a few examples. Wildfires devastate both regional and global ecosystems while causing significant structural damage, injuries, and fatalities. As a result, it is becoming increasingly vital to spot fires and track their nature, size, and consequences over wide geographical areas [2]. Early fire detection and fire risk mapping are employed to try to minimize or mitigate these impacts [3]. Terrestrial, airborne, and satellite systems are the three basic types of widely used technologies that can detect or monitor active wildfire or smoke conditions in real or near real time. These technologies are commonly equipped with optical and thermal sensors; once the data are acquired, it can be processed by suitable artificial intelligence (AI) algorithms, which are typically based on a machine learning approach [1], [4], [5], [6]. In order to recognize forest fires in their early phases and model how smoke and fires behave, these strategies rely on either hand-crafted features or sophisticated AI technologies [7]. This research concentrates on space-based detection of fire by using suitable AI algorithms for on-board wildfire detection and analysis [4], [5]. The purpose of this research is to determine whether the Distributed Satellite System (DSS) and the on-board computing resources can be employed to monitor disaster scenarios, such as wildfire monitoring, using hyperspectral satellite imagery. Moreover, the findings of such assessments may be beneficial for future Australian spacecraft missions. Hyperspectral images from the *Precursore IperSpettrale della Missione Applicativa* (PRISMA) satellite were used in this research.

In this research study, a convolutional neural network (CNN)-on-board DSS architecture for disaster event management is presented. Hyperspectral imagery is used in the proposed constellation and CNN's application for monitoring wildfires in order to provide real-time/near real-time occurrences and facilitate faster action.

II. Distributed Satellite System

DSS mission architectures are made up of numerous spacecraft/modules that interact, collaborate, and coordinate with each another, leading to the development of novel system features and/or functions [8]. According to the Research and Development (RAND) Project air force research [9].

1) Distributed constellations may weigh less and cost less to launch.
2) Distributed satellites may perform better during deployment.
3) Distributed satellite constellations may be able to fail more gracefully.
4) Distributed satellite constellations may be more survivable in an attack.

Manuscript received 25 October 2022; revised 9 December 2022; accepted 10 December 2022. Date of publication 14 December 2022; date of current version 3 February 2023. This work was supported by the SmartSat Cooperative Research Centre (CRC) and the Andy Thomas Space Foundation through the Collaborative Research Project under Grant 2.13s and Pluto Program 2022. *(Corresponding author: Dario Spiller.)*

Kathiravan Thangavel and Pier Marzocca are with the School of Engineering, RMIT University, Melbourne, VIC 3000, Australia (e-mail: kathiravan.thangavel@student.rmit.edu.au; pier.marzocca@rmit.edu.au).

Dario Spiller is with the School of Aerospace Engineering, Sapienza University of Rome, 00138 Rome, Italy (e-mail: dario.spiller@uniroma1.it).

Roberto Sabatini is with the Department of Aerospace Engineering, Khalifa University, Abu Dhabi, United Arab Emirates (e-mail: roberto.sabatini@ku.ac.ae).

Marco Esposito is with Cosine, 2171 Sassenheim, The Netherlands (e-mail: m.esposito@cosine.nl).

Digital Object Identifier 10.1109/LGRS.2022.3229173

The primary goal of DSS is to provide a more responsive and resilient solution to meet the growing demands of the research community as well as the defense sector by assisting in the monitoring and prognostication of Earth Observation (EO) missions [10] and Space Domain Awareness (SDA) missions [11], [12], [13], [14] in the promise of improving space sustainability. One of the main focuses of SmartSat Cooperative Research Centre (CRC) and Australia's space strategy is EO to improve Australia's disaster resilience by developing and deploying satellite-based information capabilities. SmartSat CRC has a dedicated Capability demonstrator I-In-The-Sky (IITS) for the same [15]. DSS is classified according to the nature of the mission and purpose they conduct. Modules performing activities in a distributed infrastructure, whether in independent satellite systems or distributed spacecraft, may include activities necessary to accomplish local objectives (i.e., those particular to each module) or a part of a global objective's functioning (i.e., specific to the infrastructure). DSS actively communicates and interacts via Intercommunication Satellite Link (ISL), where data are exchanged and processed on-board to accomplish the mission goal. This research letter proposes a constellation of Low Earth Orbit (LEO) satellites [16], [17], [18], [19], [20], [21] for EO [22]. There are two types of constellations: 1) polar and near-polar constellations and 2) Walker constellation. Walker proposed uniform constellations with the inclination criterion relaxed to lower the needed number of satellites by reducing superfluous overlap at the poles. The delta constellation, sometimes referred to as the Walker delta or a rosette, is one of the most well-known constellations [23]. The proposed DSS is considered in near-circular orbit (i.e., eccentricity is $\sim$0.001) with 500-km altitude and inclination 55° with 40 satellites equally spaced (plane spacing 36°) in four orbital planes. As we are considering a continuous coverage problem, we can disregard the values of the Right Ascension of the Ascending Node (RAAN) and Mean Anomaly. All the participants in the proposed constellation are assumed to be similar and carry the same optical payload. Satellites are often situated in orbital planes that are complementary to one another, and they communicate with each other through the Inter Satellite Link (ISL) and globally dispersed ground stations. Intersatellite communication may also be used to communicate with each other. Aiming for effective coverage across the Australian continent, the Walker scenario will be appropriate for the constellation model. On the other hand, the Walker Delta design is appealing for the current research work because of its simplicity and economic feasibility [24], [25]. The parameters i, N_s, p, and f indicate the distribution of satellites in space, where i is the inclination, N_s is the number of spacecrafts, p is the total number of orbital planes, and f is the phase difference between the participating spacecrafts in the plane, which forms the Walker Delta constellation pattern. The number of satellites in each orbit is given by $s = (N_s/p)$, where $p|N_s(p$ divisible by $N_s)$. To avoid satellite collisions, the phase difference between the neighboring spacecrafts of a specific plane is calculated using $f \times (360°/S)$, where f is an integer between 0 and $(p1)$. As a satellite observes a region on Earth, it projects a circular or rectangular imprint on the surface. The instantaneous coverage of the satellite is the distance between the satellite and a target point in the satellite field of view (FOV) region (imprint region) at a given time [26], [27]. Another fundamental parameter for the computation of the coverage is the *system-wide access*, which is the time that at least one satellite's camera can observe the area of interest (AOI) during this timeframe must be calculated in order to compute coverage and system-wide access. The corresponding percentage quantity is known as the system-wide access percentage, and it is calculated using the following equations:

$$\mathrm{SWAD} = n \cdot S_c \tag{1}$$

$$\mathrm{SD} = \mathrm{ST}_{\mathrm{Start}} - \mathrm{ST}_{\mathrm{Stop}} \tag{2}$$

$$\mathrm{SWAP} = \frac{\mathrm{SWAD}}{\mathrm{SD}} \cdot 100 \tag{3}$$

where SWAD is the system-wide access duration, n is the number of elements in system-wide access status whose value is true, i.e., 1, S_c is the spacecraft sample time, and SWAP is the system-wide access percentage. The equations that relate to the above are for the Nadir pointing, and they can also be used for systems with tracking

$$\mathrm{SWAD}_T = N \cdot S_c \tag{4}$$

$$\mathrm{SD} = \mathrm{ST}_{\mathrm{Start}} - \mathrm{ST}_{\mathrm{Stop}} \tag{5}$$

$$\mathrm{SWAP}_T = \frac{\mathrm{SWAD}_T}{SD} \cdot 100 \tag{6}$$

where SWAD_T is the system-wide access duration with tracking, N is the number of elements in system-wide access status with tracking whose value is true, S_c is the spacecraft sample time, which is considered 30 s for both the cases, and SWAP_T is the system-wide access percentage with tracking.

III. On-Board Implementation

In our previous works, a one-dimensional (1-D) CNN was investigated for spotting wildfires employing PRISMA hyperspectral imagery and encouraging results for the edge implementation on three different hardware accelerators were provided. We showed that AI-on-the-edge paradigms for future mission ideas are viable by utilizing appropriate CNN architectures and established technology to perform time- and power-efficient inferences [1], [4], [6]. The analysis in this letter was done with Level 2-D (geocoded version of the geolocated at-surface reflectance product) data. The red channel at 614.1723 nm, green at 530.66705 nm, and blue at 441.6589 nm (RGB) composite of the research area are shown in Fig. 1. For the training, we used all the PRISMA band [apart from removing overlapping bands from visible to near-infrared (VNIR) and short-wave infrared (SWIR) arrays]. However, direct information related to smoke can be retrieved by looking at single bands from VNIR bands, such as the ones around 400 nm. From SWIR bands around 2400 nm, we can have direct information on the hot pixel, which can be reasonably active fire pixels. The AI approach is used to implement automatic segmentation from the obtained image. The model, as shown in Fig. 2, was trained and validated with the sophisticated computer on the ground, and then, the trained model is tested in the hardware accelerators.

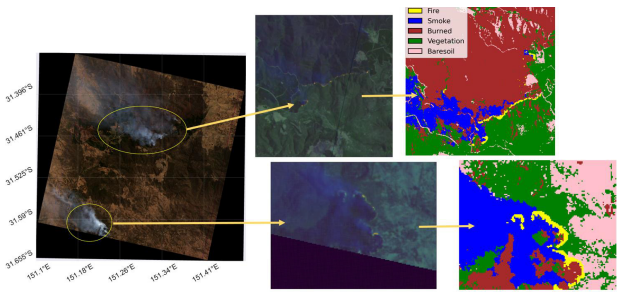

Fig. 1. Wildfire segmentation of Bushfire [1].

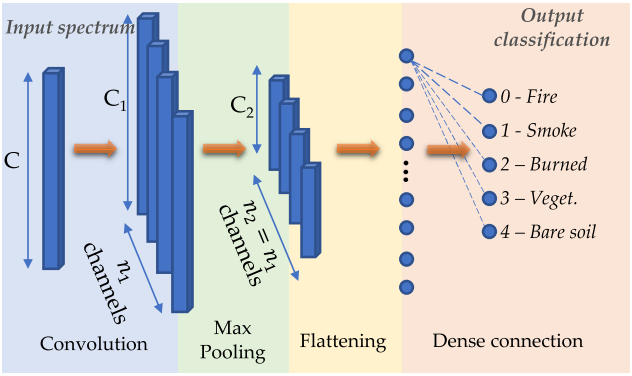

Fig. 2. One-dimensional CNN segmentation model [4].

From our previous work [1], [4], [6], all the results are in line with the spacecraft platform's total power budget; however, when it comes to CubeSats or small satellites, the Intel Movidius (inference time is 5.8 ms and power consumption is 1.4 W) and Jetson Nano (inference time is 3.4 ms and power consumption is 2.6 W) appear to be the most promising options. For our situation, we took into account the Jetson Nano and Intel Movidius on-board constellations for detecting wildfires.

IV. Results and Discussion

This simulation depicts an investigation of the AOI on the ground and conical sensors on-board a heterogeneous constellation[1] of satellites. The AOI and a satellite's conical sensor are said to have access if the ground station is within the conical sensor's FOV and the conical sensor's elevation angle (EA) with respect to the AOI. The simulation employs a constellation of 40 LEO satellites at 500-km altitude to replicate the KANYINI mission in near circular orbit with AOI. The AOI is chosen based on the wildfire occurrence in the four different continents and to generalize the simulation results. Each satellite carries a 30° FOV camera, and the entire satellite network is tasked with imaging the AOI during the sun sufficiently illuminates it. The satellite's EA with regard to the AOI should be at least 30° in order to acquire high-quality imagery with minimal atmospheric distortion. It is necessary to calculate the times when each satellite can image the site over an imposed 6-h interval. It is also necessary to calculate the percentage of time that at least one satellite's camera can observe the place during this timeframe, which

[1]*Homogeneous Constellation:* A constellation whose member spacecraft employs functional identical bus, payload, and operational characteristics (e.g., MMS and Iridium). *Heterogeneous Constellation:* A constellation whose member spacecraft employs different bus, payload, and operational characteristics.

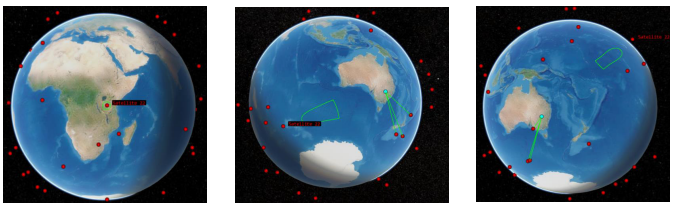

Fig. 3. Satellite FOV. (a) DSS FOV with normal configuration. (b) DSS FOV with reconfiguration at entry. (c) DSS FOV with reconfiguration at exit.

is given by SWAP in (6). The existence of the AOI within the contour indicates that it is within the FOV of the payload camera. Fig. 3(a) shows the visualization FOV of the satellite. It is necessary to calculate the system-wide access percentage, which is the percentage of time from the simulation start time to the stop time when at least one satellite can image the site, in addition to calculate the times when each camera can capture the AOI.

The satellite's default attitude arrangement is nadir pointing. Because the cameras are by default aligned with the yaw axis, they always point straight down, and the AOI is no longer visible to the cameras before their EA falls below 30°. As a result, this cumulative access percentage is constrained by the FOV of the cameras. In contrast, if the DSS can communicate and have the reactive elements in the architecture with the ISL, the satellites can be able to communicate with the nearby satellite in the constellation, and this system is said to be an intelligent DSS (i-DSS). Then, the satellites' cameras will be pointed continuously at the AOI through active attitude control adjustment; the AOI is observable as long as the Earth is not in the way, as seen in Fig. 3(b) and (c). As a result, the system-wide access percentage will now be limited by the AOI's minimum EA rather than the camera FOV. This is done based on the owner/operator requirement for the requested time period. The access periods in the former scenario began and terminated when the site entered and exited the camera's FOV. Specifically, it enters the FOV after the camera's EA exceeds 30° and exits before the camera's EA falls below 30°. The camera will be pointed at the Nadir for the rest of the period. The system-wide access for four different AOIs is shown in Table I for the NADIR pointing and tracking configuration. The table contains the latitude and longitude coordinates of the four selected AOI, expressed in World Geodetic System (WGS84). The total simulation was carried out for 21 600 s, i.e., 6 h, and the respective system-wide access with Nadir pointing and with tracking is reported. Because the cameras are firmly affixed to the satellites, each satellite must be constantly reoriented (i.e., maneuvered with the on-board actuators) along its orbit, so that its yaw axis tracks the AOI location.

The total simulation was carried out for 21 600 s, i.e., 6 h, and the respective system-wide access with Nadir pointing and with tracking is reported. Because the cameras are firmly affixed to the satellites, each satellite must be constantly reoriented (i.e., maneuvered with the on-board actuators) along its orbit, so that its yaw axis tracks the AOI location. In Fig. 4, the list of satellites that will access the AOI in the proposed constellation and the length of time that they will have access to Australia are shown, and their

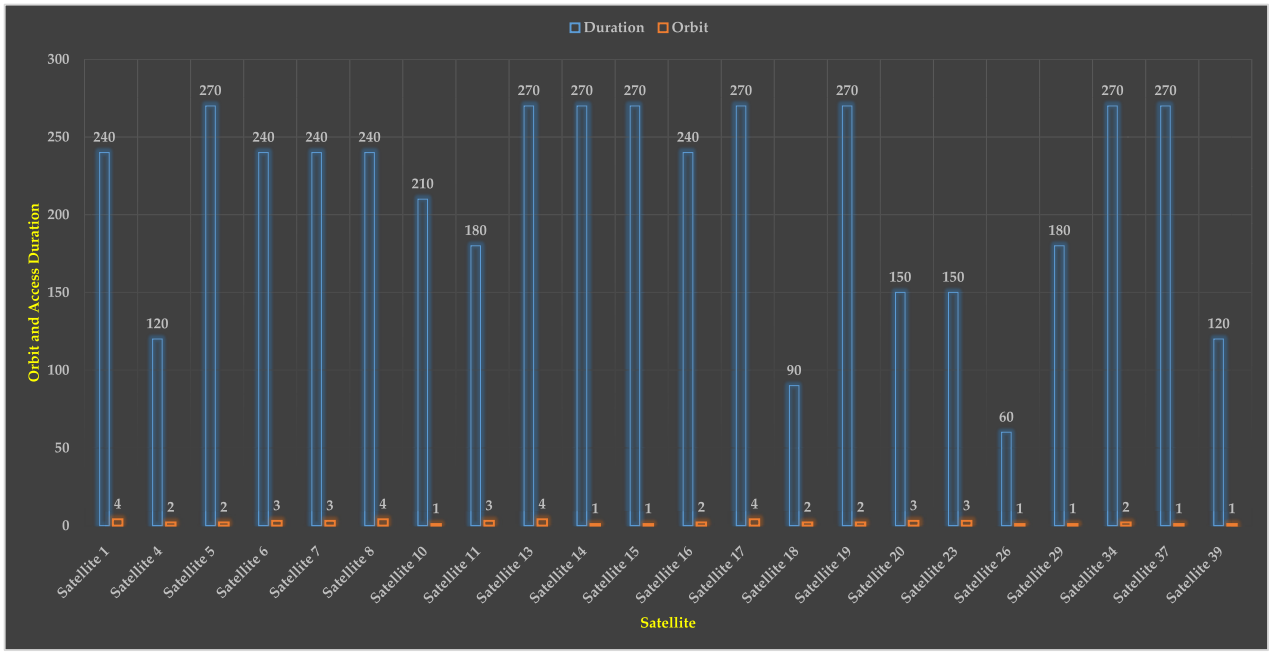

Fig. 4. Australia satellite access duration with tracking and its orbit.

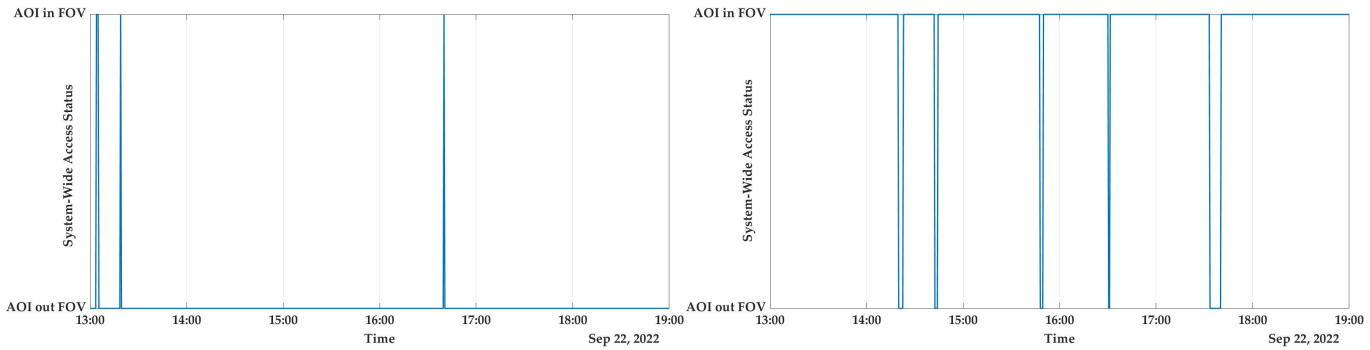

Fig. 5. Australia (a) system-wide access status and (b) system-wide access status with tracking.

TABLE I

SYSTEM WIDE COVERAGE PARAMETERS WITH RESPECT TO A SCENARIO DURATION OF 6 h, i.e., 21 600 s

Location	Latitude (deg)	Longitude (deg)	n	SWAD (sec)	SWAP (%)	N	$SWAD_T$ (sec)	$SWAP_T$ (%)
USA	44	-120.3	14	420	1.9444	699	20970	97.0833
Australia	-31.25	146.92	5	150	0.6944	691	20730	95.9722
Italy	40.1209	9.0129	10	300	1.3889	712	21360	98.8889
Africa	11.2027	17.8739	10	300	1.3889	545	16350	75.6944

corresponding orbits are presented for the simulation time. From the reported result, it is evident that with the Nadir pointing, the FOV is relatively low for most AOI, while when the active AOI pointing is done using Attitude and Orbit Control System (AOCS) on-board of the satellite, the SWAP is increased significantly and provides almost real-time/near real-time coverage, i.e., 75%–98%, which will enable the near real-time disaster response. For instance, for the Australian AOI, the obtained tracking coverage is 95.9722%, which represents a near real-time coverage for disaster events. This result can be further appreciated in Fig. 5, where the system with access status is reported for the NADIR configuration (a) and for the tracking configuration (b). In the latter case, the AOI is not visible only for very short periods of time. Finally, we can denote a decrease in performances in the African AOI, where the $SWAP_T$ is 75.6944% due to its geographical location (the distance between spacecrafts is maximum when close to the equator).

V. CONCLUSION

A low-Earth orbit DSS constellation is suggested in this research study for real-time or near real-time wildfire monitoring. It has been shown that the on-board application is feasible in terms of inference time and power consumption. The proposed satellites feature hardware accelerators on board for

edge computing, which is performed utilizing commercial off-the-shelf (COTS) components. This research study shows that real-time/near real-time monitoring is possible by altering the camera FOV, which is consistent with our earlier results. Since the DSS is always connected through ISL, it is not necessary to always do active AOCS; instead, only when one of the constellation's satellites detects a wildfire, this can communicate the other nearby satellites and perform active tracking to collect as much data as possible. The results show that we can provide almost near real-time monitoring for Australia using the chosen constellation, which has a constellation system-wide access percentage of 95.9722%. In order to enable the Trusted Autonomous Satellite Operation (TASO) in DSS, an enhanced model using CNN will be embedded within this framework in future research. In order to improve the framework, efficiently organize space-to-ground dataflow, and provide real-time/near real-time information, which could be very helpful in disaster and extreme event management, this research also suggests that hardware accelerators for on-board edge computing can be considered for future space missions. It was observed that the results were affected by the direction, in which the sensors were pointing. These outcomes are also affected by the satellite's orbits, AOI's minimum EA, camera mounting position, and placement in relation to the satellites FOV if they are not constantly pointing at the AOI. The satellites' orbits can be modified using Keplerian parameters and adjusting to the desired AOI based on owner/operator requirements. In the future, cameras can be put on gimbals that can rotate independently of the satellite, and the heterogeneous sensors in the constellation can be used to enhance the outcomes. This not only allows the satellites to look straight down, i.e., Nadir pointing, but also allows the gimbals to be adjusted to track the AOI independently, as well as the heterogeneous sensors able to provide useful data at different wavelengths.

REFERENCES

[1] D. Spiller, L. Ansalone, S. Amici, A. Piscini, and P. P. Mathieu, "Analysis and detection of wildfires by using prisma hyperspectral imagery," *Int. Arch. Photogramm., Remote Sens. Spatial Inf. Sci.*, vol. 43, pp. 215–222, Jun. 2021.

[2] M. A. Tanase, C. Aponte, S. Mermoz, A. Bouvet, T. Le Toan, and M. Heurich, "Detection of windthrows and insect outbreaks by L-band SAR: A case study in the bavarian forest national park," *Remote Sens. Environ.*, vol. 209, pp. 700–711, May 2018.

[3] B. Pradhan, M. D. H. B. Suliman, and M. A. B. Awang, "Forest fire susceptibility and risk mapping using remote sensing and geographical information systems (GIS)," *Disaster Prevention Manag., Int. J.*, vol. 16, no. 3, pp. 344–352, Jun. 2007.

[4] K. Thangavel, D. Spiller, R. Sabatini, and P. Marzocca, "On-board data processing of Earth observation data using 1-D CNN," in *Proc. SmartSat CRC Conf.*, 2022, doi: 10.13140/RG.2.2.16042.70088.

[5] D. Spiller, K. Thangavel, S. T. Sasidharan, S. Amici, L. Ansalone, and R. Sabatini, "Wildfire segmentation analysis from edge computing for on-board real-time alerts using hyperspectral imagery," in *Proc. IEEE Int. Conf. Metrol. Extended Reality, Artif. Intell. Neural Eng. (MetroXRAINE)*, 2022, pp. 725–730, doi: 10.1109/MetroXRAINE54828.2022.9967553.

[6] D. Spiller, S. Amici, and L. Ansalone, "Transfer learning analysis for wildfire segmentation using prisma hyperspectral imagery and convolutional neural networks," in *Proc. 12th Workshop Hyperspectral Imag. Signal Processing: Evol. Remote Sens. (WHISPERS)*, Rome, Italy, Sep. 2022, pp. 1–5.

[7] P. Barmpoutis, P. Papaioannou, K. Dimitropoulos, and N. Grammalidis, "A review on early forest fire detection systems using optical remote sensing," *Sensors*, vol. 20, no. 22, p. 6442, Nov. 2020.

[8] A. H. Poghosyan et al., "1 unified classification for distributed satellite systems," 2016.

[9] R. Preston, *Distributed Satellite Constellations Offer Advantages Over Monolithic Systems*. Santa Monica, CA, USA: RAND Corporation, 2004.

[10] A. C. Kelly and E. J. Macie, "The A-Train: NASA's Earth Observing System (EOS) satellites and other Earth observation satellites," in *Proc. 4th IAA Symp. Small Satell. Earth Observ.*, Berlin, Germany, Apr. 2003, p. 4. [Online]. Available: http://virbo.org/virbo/images/5/5f/NSF_Smallsat_backup_A-train.pdf

[11] R. Sabatini, "Aerospace cyber-physical and autonomous systems," 2020. [Online]. Available: https://www.researchgate.net/publication/341787434_Aerospace_Cyber-Physical_and_Autonomous_Systems

[12] J. Utzmann et al., "Space-based Space Surveillance and Tracking demonstrator: Mission and system design," in *Proc. Int. Astron. Congr. (IAC)*, vol. 3, 2014, pp. 1648–1654. [Online]. Available: https://www.researchgate.net/publication/288588749_Space-based_Space_Surveillance_and_Tracking_demonstrator_Mission_and_system_design

[13] M. K. Ben-Larbi et al., "Towards the automated operations of large distributed satellite systems. Part 1: Review and paradigm shifts," *Adv. Space Res.*, vol. 67, no. 11, pp. 3598–3619, 2021.

[14] M. K. Ben-Larbi et al., "Towards the automated operations of large distributed satellite systems. Part 2: Classifications and tools," *Adv. Space Res.*, vol. 67, no. 11, pp. 3620–3637, 2021.

[15] SmartSatCRC. *I-in-The-Sky*. Accessed: Sep. 21, 2022. [Online]. Available: https://smartsatcrc.com/capability-demonstrators/i-in-the-sky/

[16] O. Brown and P. Eremenko, "The value proposition for fractionated space architectures," *Science*, vol. 4, p. 23, Sep. 2006.

[17] B. Heydari, M. Mosleh, and K. Dalili, "From modular to distributed open architectures: A unified decision framework," *Syst. Eng.*, vol. 19, no. 3, pp. 252–266, May 2016.

[18] J. Guo, D. C. Maessen, and E. K. Gill, "Fractionated spacecraft: The new sprout in distributed space systems," 2009. [Online]. Available: https://www.semanticscholar.org/paper/Fractionated-spacecraft%3A-The-new-sprout-in-space-Guo-Maessen/ae8174f33a9a6f412271b1122c3c80608237df31

[19] O. C. Brown and P. Eremenko, "Fractionated space architectures: A vision for responsive space," 2006. [Online]. Available: https://www.semanticscholar.org/paper/Fractionated-Space-Architectures%3A-A-Vision-for-Brown-Eremenko/33710d0dcf5ebc9228b6f968fe6fe3ccf9c5e79a

[20] B. S. Schwarz, "Fractionated satellites: A systems engineering analysis," Ph.D. thesis, Dept. Eng. Environ., Univ. Southampton, Southampton, U.K., 2014, p. 176. [Online]. Available: https://eprints.soton.ac.uk/370544/

[21] B. Yaglioglu and J. Wang, "Cluster flying configuration evaluation in the case of fractionated spacecraft architecture," 2010. [Online]. Available: https://www.researchgate.net/publication/309512577_Cluster_Flying_Configuration_Evaluation_in_the_Case_of_Fractionated_Spacecraft_Architecture

[22] L. Qiao, C. Rizos, and A. Dempster, "Design and analysis of satellite orbits for the Garada mission," 2011. [Online]. Available: https://www.researchgate.net/publication/235935851_Design_and_Analysis_of_Satellite_Orbits_for_the_Garada_Mission

[23] J. G. Walker, "Circular orbit patterns providing continuous whole earth coverage," Royal Aircraft Establishment Farnborough, Farnborough, U.K., Tech. Rep., 1970.

[24] J. G. Walker, "Satellite constellations," *J. Brit. Interplanetary Soc.*, vol. 37, p. 559, 1984. [Online]. Available: https://ui.adsabs.harvard.edu/abs/1984JBIS...37..559W/abstract

[25] J. R. Wertz, *Mission geometry; Orbit and Constellation Design and Management. Space Technology Library*, 2001. [Online]. Available: https://link.springer.com/book/9780792371489

[26] R. P. Perumal, H. Voos, F. D. Vedova, and H. Moser, "Comparison of multidisciplinary design optimization architectures for the design of distributed space systems," in *Proc. 71st Int. Astron. Congr.*, 2020. [Online]. Available: https://orbilu.uni.lu/handle/10993/44677

[27] R. P. Perumal. (2021). *Development of a Decision Support System for Incorporating Risk Assessments during the System Design of Microsatellites—Pandi Perumal Raja*. University of Luxembourg. [Online]. Available: https://orbilu.uni.lu/handle/10993/48261

Open Access funding provided by 'Università degli Studi di Roma "La Sapienza"' within the CRUI CARE Agreement